Modeling, Simulation, and Visualization Environment to Support Independent Verification and Validation of Artemis I Separation Events

Paul Tartabini [(1)], Brett Starr [(1)], Jeremy Shidner [(2)], Rafael Lugo[(1)], Benjamin Tackett[(2)], Esther Lee[(1)], Scott Angster[(2)], Bandu Pamadi[(2)], Peter Covell[(2)], Tannen VanZwieten[(3)]

[(1)] NASA Langley Research Center, Hampton, VA, Paul.V.Tartabini@nasa.gov
[(2)]Analytical Mechanics Associates, Hampton, VA,, Jeremy.D.Shidner@nasa.gov
[(3)]NASA Engineering and Safety Center, Kennedy Space Center, FL, Tannen.VanZwieten@nasa.gov

ABSTRACT

On November 16, 2022, the Space Launch System (SLS) successfully completed its debut mission in support of NASA's Artemis I mission. A decade prior to this, the NASA Engineering and Safety Center initiated a technical assessment to develop and maintain the capability to model and simulate the newly developed launch vehicle's ascent and separation events independent from the SLS Program. The assessment team created an independent multi-body six degree-of-freedom (6-DOF) end-to-end simulation that was used to perform in-depth analyses of ascent and critical separation events. A visualization environment was used to compute separation clearances. This independently developed suite of tools provided high-fidelity verification of critical analyses (including assessment of design requirements) and provided the capability for analyses to be performed on an as-needed basis without drawing on SLS Program resources. This paper will present an overview of the simulation and separation analysis capability and discuss the integration of key simulation models such as flexible body dynamics, slosh dynamics, separation mechanisms, multi-body aerodynamics, and environmental models. Additional details are provided about challenges that were addressed across the decade of analysis that was conducted.

1 Introduction

On November 16, 2022, NASA successfully flew the Artemis 1 mission, marking the first flight of the Space Launch System (SLS). The flight was a culmination of a decade of design, development and testing that required careful integration with multiple industry partners and multiple programs (SLS, Orion, and Exploration Ground Systems). In the years leading up to the flight, technical integration among these different entities was considered one of the top risks for the Agency. As a mitigation to this risk, the NASA Engineering and Safety Center (NESC) initiated an effort to create an independent modeling and simulation capability in support of SLS and the Orion Multi-Purpose Crew Vehicle (MPCV). Established by NASA after the Space Shuttle Columbia accident of 2003, the NESC serves as an independent, Agency-wide engineering resource that performs assessments of its high-risk projects to ensure safety and mission success [1]. To fulfill this mission for SLS, the NESC assembled a dedicated team of subject matter experts, independent from the SLS Program (SLSP), to develop an end-to-end simulation of the Artemis I SLS ascent trajectory and to perform detailed analyses of the critical separation events. Results of these analyses were then used to provide independent verification and validation (IV&V) of ascent trajectory and separation clearance analyses performed by the SLS Program.

This independent modeling and simulation effort was viewed by the NESC as a long-term commitment and investment to develop and maintain an in-house expertise and familiarity with the critical SLS flight systems and trajectory phases throughout design, verification, and flight readiness cycles. By initiating it early in the SLS development, the assessment team was well positioned to identify unanticipated issues or problems related to vehicle design and analysis that frequently occur due to the highly integrated nature of these new systems. In addition, having an independent integrated simulation that was mature and verified ensured that the NESC could rapidly address potential issues throughout the program lifecycle by avoiding the long lead times typically associated with the development of a complex flight simulation.

This paper provides an overview of the tools used to conduct independent modeling and simulation of Artemis 1 separation events and highlights the challenges and lessons learned across a decade of analysis. An overview of each of the tools along with the process flow and key components of maintaining independence from the Program's baseline tool set is provided. In addition, each of the separation analyses conducted is discussed, making note of key models incorporated for each event and unique challenges that were addressed.

2 Tools and Approach

The core of the independent modeling and simulation capability developed for SLS is a multi-body six degree-of-freedom (6-DOF) end-to-end trajectory simulation that includes all the major events occurring during the Artemis I ascent trajectory, from liftoff until separation of the Interim Cryogenic Propulsion Stage (ICPS) from the Core Stage (CS) after main engine cutoff (MECO). Figure 1 highlights the significant ascent events; all were modeled in the simulation except for the SRB descent trajectories after booster separation. To maintain independence from the project, the vehicle and mission-dependent simulation models (e.g., aerodynamics, mass properties, flight control software, etc.) were received in their raw data form directly from the engineering teams that developed them. These models were implemented completely independent of any project simulation code or input files, allowing the team to develop their own modeling assumptions when working through the implementation details. This positioned the NESC and Program teams such that the results and conclusions were developed independently, allowing for implementation assumptions to be challenged where results differed.

Once the end-to-end simulation was developed, additional modeling fidelity was added to perform detailed assessments of the separation events numbered in Figure 1, including analysis of liftoff clearance between the vehicle and ground support structures, solid rocket booster (SRB) separation from the CS, Service Module (SM) panel jettison, separation of the ICPS from the CS, and MPCV/ICPS separation after trans-lunar injection. To support these assessments, numerous unique simulation models were developed and integrated into the standard suite of simulation models to address and resolve key concerns specific to each separation event. When appropriate, additional bodies were simulated to compute the trajectories of separating stages or elements, and the multi-body dynamics results were passed to a visualization tool to compute relative distances and check for recontact. Because of the end-to-end nature of the simulation, each separation analysis that was performed included the state information that was based on the trajectory and uncertainty effects from launch until separation. Details are provided about other challenges that were addressed, including the use of a convex hull to reduce computational time for clearance calculations, the impact of structural flexibility on tight clearances during booster separation, and the capability to simulate failure scenarios.

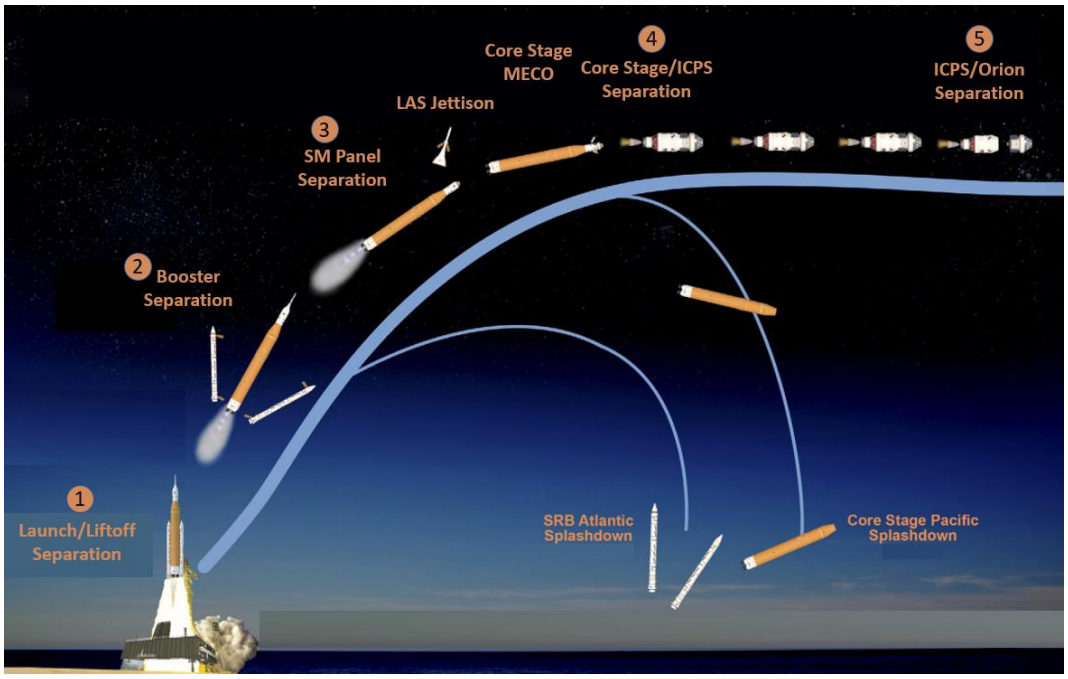

Figure 1. Artemis I SLS ascent trajectory.

2.1 POST2 Trajectory Simulation Architecture

The scope of the NESC assessment included the development of a 6-DOF simulation built independently from the SLS Program that modeled the elements of the SLS launch vehicle ascent sufficiently to assess its performance from launch to MPCV separation from the ICPS. The trajectory and separation analyses were conducted using this simulation.

The NESC independent simulation architecture used for this effort is the Program to Optimize Simulated Trajectories II (POST2). POST2 is a NASA Class D (Non-Safety Critical) generalized point mass, rigid body, discrete parameter targeting and optimization trajectory simulation program based on the POST software developed in the 1970s at NASA Langley Research Center in partnership with the Martin Marietta Company. Development of POST2, began in the 1990s to expand the modeling capability and update the internal software architecture to be primarily C-based. POST2 has been used successfully to solve a wide variety of atmospheric ascent and re-entry problems, as well as exo-atmospheric orbital transfer problems using 3-DOF or 6-DOF trajectory simulations [2],[3],[4]. It contains many generalized models (e.g., atmosphere, gravity, propulsion, and navigation system) that can be leveraged to simulate a wide variety of missions. Alternatively, user-supplied code can be incorporated to provide vehicle-specific aerodynamic data, atmosphere models, optimization capability, and onboard flight/mission-specific software. Capability is also included to support Monte Carlo dispersion analysis.

POST2 controls simulation flow by using trajectory phases triggered by discrete user-defined event criteria. Complex trajectory sequences can be simulated using Boolean logic with real, integer, or variable (instead of constant) criteria to trigger events. POST2 can also activate and/or deactivate any number of vehicles at any event during the trajectory, and initialize multiple vehicles using state information derived from another existing vehicle in the simulation (e.g. booster state initialized from core vehicle state at separation event).

Both built-in and user-provided configurable models for different subsystems were used (with appropriate input values) for the NESC ascent trajectory simulation (see Fig. 2). The simulation

included environment models (e.g., gravity, atmosphere), vehicle models (e.g., aerodynamics, thrusters), and models delivered by the SLSP (e.g., G&NC, actuating gimbals, throttle, SRB). Comparisons between the nominal trajectory outputs from the various SLSP simulations were performed regularly. Differences in models, implementation, and subsequent results were identified and noted during these comparisons. NESC and SLSP engineering results were determined to be within tolerance for each metric of interest during analysis cycles completed prior to launch. The model manifest used in the NESC analysis is shown in Table 1.

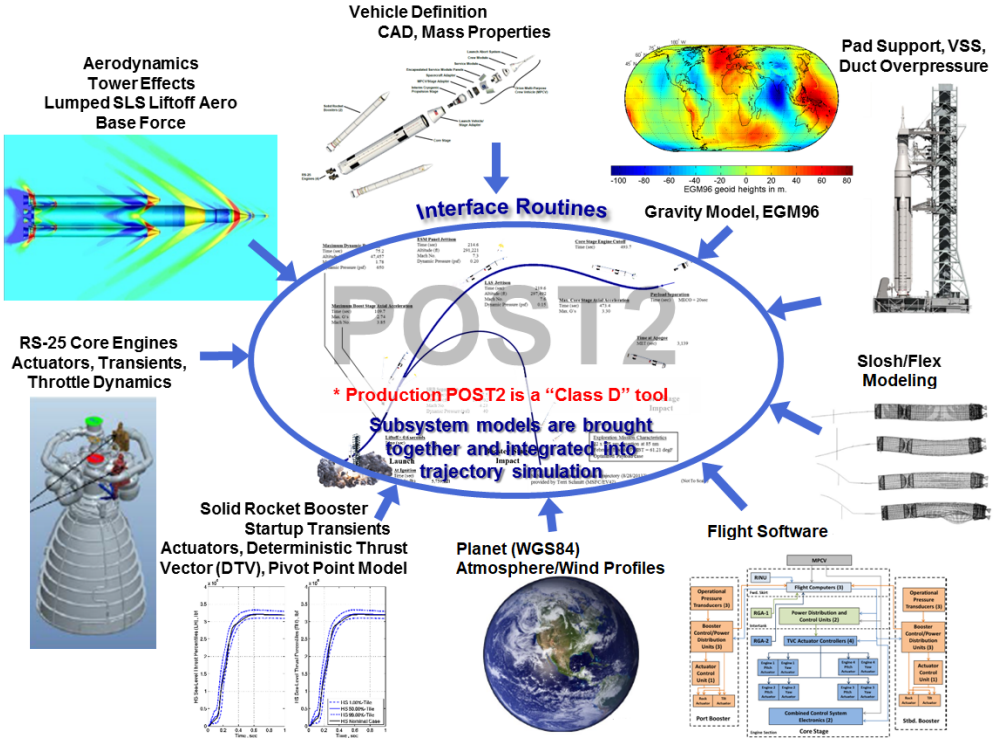

Figure 2. POST2 simulation architecture

Table 1. Simulation Models

Stage Level Models		Vehicle Level Models	
SRB	Steady State and Tailoff Thrust Profile Deterministic Thrust Vector and Pivot Point Thrust Vector Control Actuators 6-DOF Dry Mass Properties Propellant Sequential 6-DOF Mass Properties Booster Separation Motor Performance	Environment	Global Reference Atmosphere Model (GRAM) Atmospheric Thermodynamic Properties Measured Wind Profiles
Core Stage	Engine Performance Models Engine Startup, Shutdown Transients Thrust Vector Control Actuators LH2 and LOX Tank Slosh Separation Mechanisms 6-DOF Dry Mass Properties Propellant Sequential 6-DOF Mass Properties Core Stage LH2 and LOX Tank Venting	Aerodynamics	Liftoff and Tower Effects Ascent Aerodynamics Base Force Effect SRB Separation Aerodynamics (nearfield/interference, farfield aero) SM panel separation Aerodynamics (Nearfield/Interference, Farfield) Core Stage Reentry Aerodynamics Aerodynamics of Core Stage Breakup Pieces
ICPS	Engine Performance Models Separation Mechanisms LH2 and LOX Tank Slosh 6-DOF Dry Mass Properties Propellant Sequential 6-DOF Mass Properties	Structural	Nominal Vehicle Flexible Modes Vehicle dispersed flex modes Mobile Launcher Base Flexible Modes
MPCV	SM Panel Separation Mechanisms MPCV Tank Slosh 6-DOF Dry Mass Properties Tank Fluids 6-DOF Mass Properties	GN&C	SLS GN&C Flight Software Models Artemis 1 GN&C Parameters Redundant Inertial Navigation unit (RINU) Rate Gyroscope Assembly (RGA)
LAS	6-DOF Mass Properties	Geometry Models for Clearance Calculations	Mobile Launcher Base Keep Out Zone Mobile Launcher Tail Service Mast (TSM) Keep Out Zone Mobile Launcher Tower Keep Out Zone Lightning Protection System (LPS) Keep Out Zone SLS Vehicle Outer Mold Line and Convex Hull SRB Outer Mold Line Launch Vehicle Stage Adapter (LVSA) Inner Mold Line ICPS Computer Aided Design (CAD) Geometry MPCV Spacecraft Adapters CAD

Continuous Integration and Testing. Continuous integration and testing were implemented with the NESC POST2 simulation architecture using Subversion (SVN) and Jenkins/Piper. SVN is an open-source software version control system [5]. SVN was used for version control of both the POST2 core codebase, as well as the SLS simulation-specific codes. This approach provides access to any version of the source code and/or simulation models used throughout the duration of the assessment. SVN was used for version control of both the POST2 core codebase, as well as the SLS simulation-specific codes, by storing both in centralized software "repositories." In this way, the POST2 core software could be developed, updated, and maintained independently of the SLS-specific code. Users could then "check out" the simulation repositories (that is, make a local copy), make necessary modifications, and commit those modifications back to the centralized repository. This permits other users to quickly obtain those changes in their local simulation check-outs.

Jenkins is an open-source continuous integration software platform [6] used to drive the automated regression testing of the POST2 core codebase and the SLS simulation-specific codes. Scripting within Jenkins implements POST2-software-specific testing needs, such that any modifications to the POST2 core or SLS simulation codebases automatically trigger a suite of hundreds of regression and unit tests that ensure code modifications do not appreciably change the expected behavior of the code. This automated testing provides simulation users and developers with a single method of maintaining codebase integrity.

Modular Software Interfaces. SLS-specific codes were modularly integrated with the POST2 core codebase primarily via the use of function pointers, which are C programming language constructs that permit the user to execute custom functions at various pre-specified locations in the codebase. In the case of its implementation in POST2, function pointers can be interpreted essentially as "sockets" into which users can "plug in" custom codes. For example, SLS aerodynamics models are hooked into the POST2 core code via the core aerodynamics function pointers. Use of these function pointers permits users to maintain and interface their own codes without having to modify POST2 core code.

Flight Software/Hardware Interfaces. SLS-specific flight software and hardware models (e.g., Guidance, Navigation, and Control (GN&C), Redundant Inertial Navigation Unit (RINU), Rate Gyro Assemblies, gimbals, and throttle) were delivered by the SLS Program to ensure that the various IV&V simulation codebases shared the same GN&C and hardware codes, while still maintaining an appropriate level of IV&V. Both native C language and Matlab Simulink models (autocoded to C) were implemented in the POST2 simulation via its flight software interface. This interface is a POST2 model that permits external codes to be called at user-specified frequencies and order. To speed up run time, the model calls are interpolated to the correct timepoints if running at different frequencies than the simulation, e.g. the RINU runs at 4800 Hz due to high rate filters while the simulation timestep is only 200 Hz, requiring 24 interpolated RINU time points between integration steps.

Higher Fidelity Modeling. Other models that provided much more detailed insight to the SLS vehicle dynamics include multibody interactions (e.g., spring-dampers, contact forces, connecting joints), gravity harmonics, 3rd body gravity perturbations of the sun/moon, spring-damper slosh, and flexible body modeling. Some of these higher fidelity models are discussed later in this report. Modeling of push-off springs was performed by a generalized multibody line system in POST2 that specifies stiffness, damping, and pre-loads for springs. Such springs were used in the SM panel separation, ICPS-core stage separation, and ICPS-MPCV separation, as described later in this report. An 8x8 gravity harmonics model was used that was derived from the Grace Gravity model [7] to better capture orbital perturbations during coast phases. Slosh was modeled via a spring-

damper slosh model parameterized by tank location, non-linear wave amplitude damping effects, and frequency scaled by axial acceleration during flight. Slosh was modeled for the Core and ICPS stage liquid hydrogen (LH2) and liquid oxygen (LOX) tanks as well as the MPCV SM tanks. The flexible body modeling integrated the modal force derived from the thrust, SRB chamber expansion forces, slosh forces, and tail-wags-dog gimbal forces to derive harmonic motion at the SLS sensor and gimbal locations for an integrated feedback loop.

Monte Carlo Analysis. Traditionally, simulations perform Monte Carlo analysis by wrapping scripts around the execution of the simulation, varying input parameters via the scripted interface, running the simulation, and finally collating outputs for results presentation. The SLS simulation used an approach that integrated the parameter dispersions and output processing directly into the POST2 software to enable better management and change tracking of the Monte Carlo processes. This approach reduced Monte Carlo run complexity by no longer requiring custom scripts, provided a generalized run capability for any computing cluster, and simplified output processing for discrete Monte Carlo data and time history profiles.

2.2 Visualization and Calculation of Separation Clearances using EVE

To assess separation performance, POST2 simulation results were post processed in the Exploration Visualization Environment (EVE) to visualize motion, compute separation clearances, and detect recontact occurrences, if any, between the separating stages or elements. EVE is a NASA Class D software system that follows NPR 7150.2 [8] processes and is specifically designed to integrate time-based dynamics data with detailed graphical models in a full-scale virtual environment. To enable the user to explore and analyze the data, EVE is built on several components to facilitate the integration of simulation and vehicle geometry data within a visualization scene, enable the user to navigate the scene in time and space, analyze object relationships, and display and output resultant analyses. Vehicle and stage geometry mesh models can be added to the scene based on polygonal model industry standards such as those typically available in computer aided design (CAD) systems. These three-dimensional (3D) geometry models are then moved within the scene using time-based position and orientation data exported from the POST2 simulation. Within EVE, the user can navigate by running time forward or backward at any time rate to look in detail at millisecond-scale events such as thruster firing data, or at longer time scales (on the order of seconds, minutes, or even much longer) so that entire separation events, including the time leading up to and following separation, can be viewed together in context. It is also possible to navigate spatially by “tethering” to any object within a scene to move with that object and get different perspectives of the relative motion.

EVE also has the capability to analyze the proximity of objects, down to the polygonal level of the geometry models integrated into a visualization scene. The distance between objects or sets of objects is computed, and the location of the minimum distance point on each object or set of objects is determined. If a collision is detected, EVE provides the point of intersection. Proximity analyses can be run interactively as the user is navigating the scene in time and space. Alternatively, it can be run in a batch processing mode which enables EVE to rapidly analyze sets of data files, such as the results of a Monte Carlo analysis.

2.3 POST2/EVE Integration

The process used to evaluate the SLS Program’s separation results is shown in Figure 3. At the center of the process is the EVE clearance calculation engine. Monte Carlo results from POST2 provide the position and orientation states of each separating vehicle or stage, and the clearance geometry models are derived from SLS CAD models.

The POST2 ascent trajectory and separation Monte Carlo analyses were performed by running 2000 dispersed cases using a set of input uncertainties and dispersions on parameters associated with the following models: aerodynamics for ascent, liftoff, and base force; CS engine and SRB thrust vector control systems; SRB thrust, mass flow rate, chamber pressure and exit area; CS engine thrust and specific impulse; CS and SRB thrust misalignments; dry mass and propellant mass properties (mass, center of gravity locations and moments and products of inertia); propellant slosh for CS, ICPS and MPCV (slosh mass, location, damping and frequency); flexible body effects (modal frequencies, mode shapes/slopes); and dispersed winds and atmosphere tables. Combined, there were over 500 different dispersions and uncertainties in the baseline ascent Monte Carlo analysis. This total was larger for most of the separation analyses, since they typically had additional uncertainties that were specific to the separation event under consideration. Some of the unique uncertainty models are discussed in the sections below covering individual separation analyses.

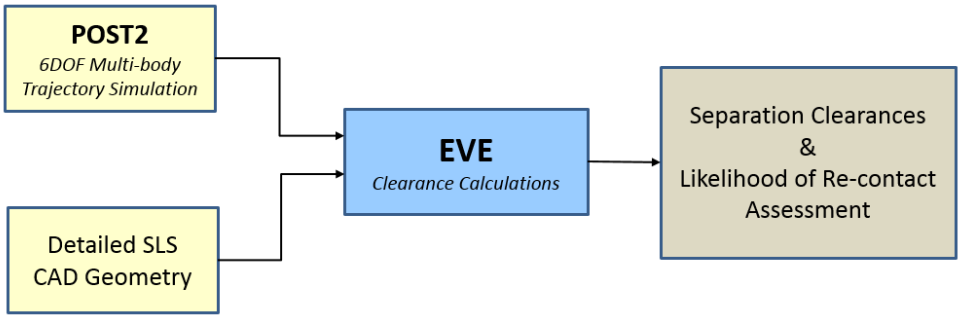

Figure 3. Analysis process used to compute separation clearances.

3 Separation Analyses

3.1 Liftoff Separation

The liftoff of the SLS vehicle from its Mobile Launcher (ML) and ascent through its Lightning Protection System (LPS) presents multiple opportunities for contact between the vehicle and ground support/launch structure. Specifically, the vehicle's nozzles must rise out of cutouts in the ML base and above vehicle support posts (VSP) without contact. As the vehicle lifts off the pad, it must also pass by the Tail Service Mast (TSM) on the ML base and then ascend past the ML tower without contact. As the vehicle clears the tower and performs a roll and pitch maneuver, it must pass through the LPS above the tower. A graphical representation of the SLS vehicle on the ML is shown in Figure 4 along with an aerial photograph of the LPS.

For separation clearance analyses, 3D geometry models of keep out zones (KOZ) are defined that encompass the ML (including the base, TSM, and tower) and the LPS structures, for the purpose of including additional clearance margins beyond the physical structures. Figure 5 provides a representative EVE proximity analysis where the different KOZ geometries are shown for the ML base (red), TSM (yellow), and tower (brown) and for the LPS (blue). The yellow lines represent the closest polygon-to-polygon point as computed by EVE from the SLS vehicle to the four KOZ geometries of interest. No part of the SLS vehicle should touch or intrude into any of these keep out zones during lift-off. To reduce geometry model complexity the SLS vehicle was represented as a convex hull that encompassed the SLS outer mold line. The convex hull (also shown in Fig. 5) decreased EVE run time without compromising the integrity of the proximity analysis.

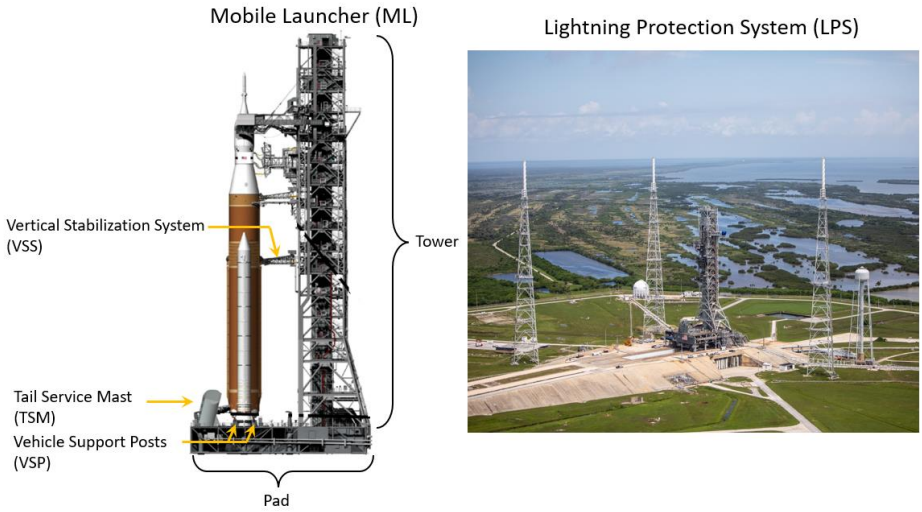

Figure 4. Key features of ML (left) and aerial view of LPS (right).

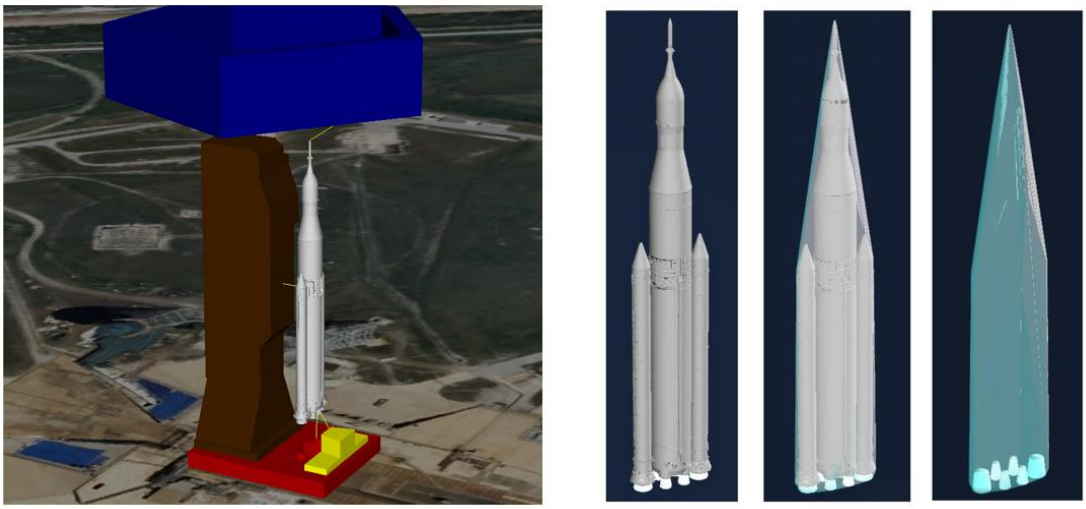

Figure 5. Keep out zones encompassing the lightning protection system and ML base, tower, and TSM (left). Convex hull representation of SLS vehicle (right).

The NESC team used the POST2 flight simulation to determine the state information during the SLS liftoff event from CS engine ignition through LPS clearance. Simulation models were added to improve the fidelity of the liftoff analysis. First, a low altitude wind database was added to provide a more accurate estimate of wind variation at the pad height. Additional forces and moments imparted on the vehicle as it lifts off were modeled, including those from the VSPs and umbilicals as well as forces/moments due to pressure oscillations acting on the SRB structure during SRB ignition. These added details affect the vehicle's flexible body response and the rate at which the vehicle clears the launch platform, which improve the accuracy of the vehicle dynamic response and liftoff clearances.

In the nominal SLSP ascent profile, at ~0.25 seconds after SRB ignition, the vehicle's thrust exceeds its weight and the vehicle begins ascending from the launch pad. At ~1.3 seconds, the SRB nozzles clear the VSP, and at ~7 seconds, the vehicle clears the tower (350-foot height) and begins the roll/pitch maneuver toward the East. At ~9 seconds, the LPS is cleared. During the liftoff event, the critical drivers to vehicle motion are aerodynamic forces and moments due to thruster misalignments and winds. Figure 6 shows a comparison of NESC simulation results to the SLSP nominal ascent. The nominal clearance time histories for the undispersed liftoff trajectory using the

KOZ geometries discussed previously are shown. The SLS clears the base and TSM at ~1.3 seconds, the tower at ~7 seconds, and the LPS at ~9 seconds (represented by red circles in the figure). The NESC performed additional sensitivity studies to evaluate the effects of extreme winds, CS engine out failures, and CS and SRB TVC hard-over failures. Dispersed Monte Carlo analysis was used to generate statistics of interest related to each KOZ clearance.

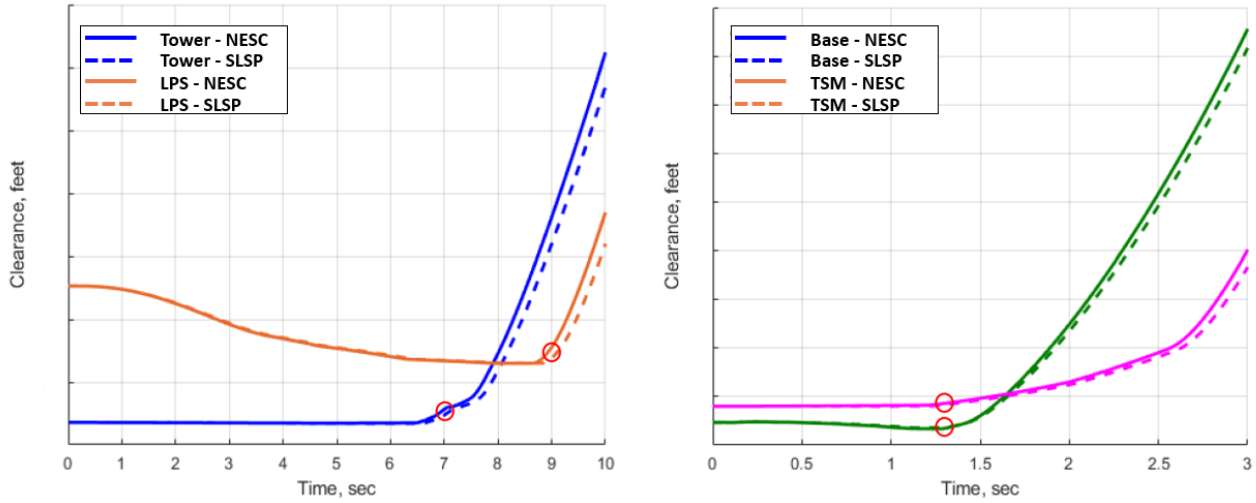

Figure 6. Comparison of separation clearances between launch vehicle and keep out zones

3.2 SRB Separation

SRB separation occurs approximately two minutes into the SLS ascent, at an altitude of roughly 160,000 feet, and near Mach 4.2 (See Fig. 7). The separation event is triggered when the sensed chamber pressure in both SRBs drops below 50 psia. After a short delay, forward and aft separation mechanisms are released and eight booster separation motors (BSMs) are fired on each SRB (four on the forward frustrum and four on the aft skirt) to provide the lateral separation force to push the booster out and away from the CS. The relative axial acceleration between the CS and SRBs is caused by the net differences in thrust levels, with CS engines (CSEs) operating at nominal thrust and SRBs thrust tailing off.

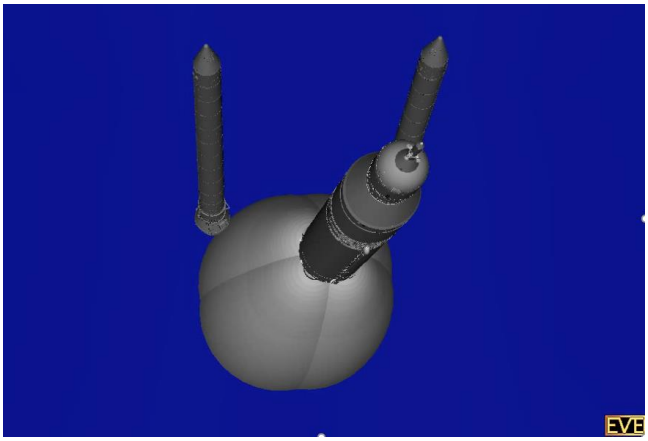

Figure 7. EVE Screenshot: Separation of SRBs from CS.

The primary objective of the SRB separation analysis was to estimate separation clearances, defined as the minimum distance between any part of the CS and any part of the SRB. There were 35 different clearance calculations metrics defined for SRB separation analyses that covered all the relevant combinations of vehicle geometry. These included “macro” clearances from any point on

the CS to any point on each SRB, and “micro” clearances, between different parts of each element. These clearance calculations cover all the relevant combinations of vehicle geometry and provide a comprehensive assessment of booster separation performance and the likelihood of recontact. A screenshot from a representative EVE analysis is shown in Fig. 8.

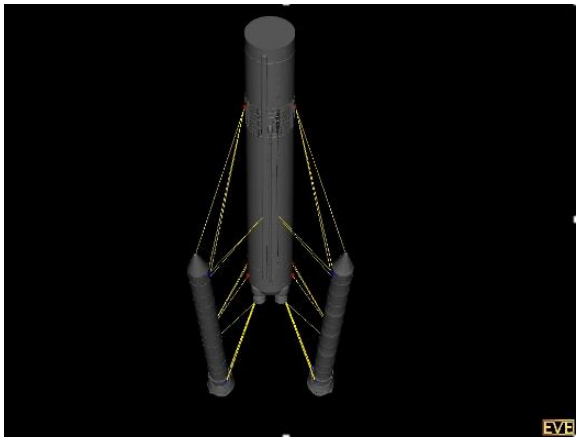

Figure 8. Screenshot of EVE performing an SRB separation clearance analysis

To model SRB separation in the POST2 simulation, the 6-DOF ascent simulation was propagated to the start of the SRB separation sequence (when the chamber pressure sensors in both SRBs indicate the booster thrust is beginning to tail off). At that point, two additional vehicles defining the SRBs were initiated and attached at the proper locations relative to the CS. Linear spring-dampers were used to model the four individual attachment points for each SRB (one forward attachment and three aft strut attachments). After a pre-determined delay to arm pyrotechnic systems, null SRB nozzles, and allow thrust and dynamic pressure to decrease, the separation command signal is sent to release the boosters and ignite the BSMs. Nominally, each BSM fires for ~1 sec, which translates to approximately 15-20 feet of axial separation of the SRBs relative to the CS. The separation clearances were estimated during this period and aerodynamic forces/moments were found to be sufficiently high to impact critical separation clearances. When the SRBs move further away from the CS, they come under the influence of CSE plumes which impact the SRBs and produce significant forces/moments on them. However, by that time the SRBs are moving away from the CS with very little possibility of any recontact due to CSE plume impingement.

To account for this complex flow field, the Artemis I SRB separation aerodynamic database was developed using a similar approach as the heritage Space Shuttle booster separation database that was entirely generated using proximity wind tunnel test data. For Artemis I, inviscid Euler and viscous Navier Stokes CFD were used to generate the booster separation database, and proximity wind tunnel test data was used for CFD code validation and to estimate database uncertainties. A typical CFD generated aerodynamic flow field around the SLS is shown in Figure 9. The Artemis I SRB separation aerodynamic database is a large, complex, multi-dimensional database providing total aerodynamic coefficients for the CS and both SRBs during separation. The 8-dimensional database is a function of CS angle of attack and side slip, three relative separations in axial, lateral and transverse directions, two relative angular orientations in pitch and yaw, and the average BSM thrust coefficient. To reduce POST2 run time, the database was translated into C code and compiled directly into the POST2 executable.

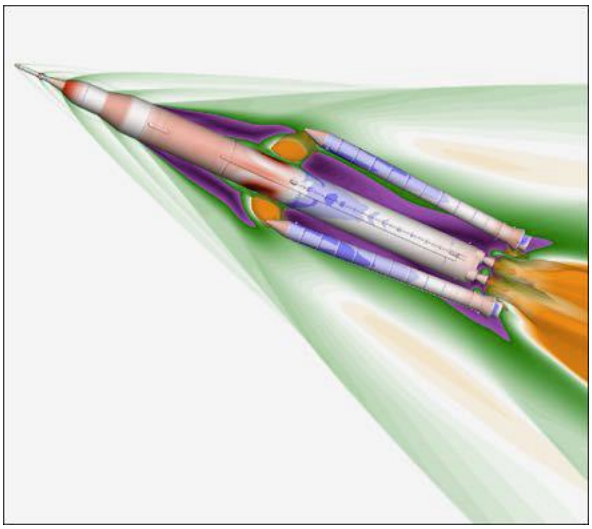

Figure 9. Aerodynamic flow field around SLS Artemis Vehicle.

To verify that the likelihood of any recontact is below the required threshold, Monte Carlo analyses were performed using the typical set of ascent uncertainties as well as additional booster separation uncertainties, and separation clearances between the CS and each SRB were calculated for each dispersed trajectory. Some of the additional uncertainty models that were specific to SRB separation included: dispersed SRB steady state and tail-off thrust profiles; dispersed BSM thrust vectors (magnitude and direction); booster chamber pressure sensor measurement errors; SRB separation aerodynamic uncertainties, uncertainties in the location and length of aft strut attachments, uncertainties in structural flexibility parameters, BSM ignition delays, latencies in individual attachment bolt release times, and uncertainties in disconnect forces due to breakwires and disengagement of pyro lines as the SRBs separate. With the combined ascent and booster separation uncertainties, there were nearly 800 dispersed variables in the POST2 booster separation Monte Carlo analyses.

Uncertainties were also accounted for in the EVE clearance calculations. First, because aft attachment strut stubs on the CS and each SRB can freely articulate after they are severed at separation, “swept” strut geometries were used to compute aft strut clearances. These swept geometries were modeled as solid surfaces that envelope the full articulation limits of the struts. This ensured that the uncertainty of how the struts could behave after the aft attachment bolts have been severed was captured in the clearance analysis. A second detail that was important to include was the effect of vehicle flexibility on the CS and SRBs. By modeling flexible body dynamics during separation, it was possible to evaluate how linear and angular displacements due to flexing motion at each attach point and along the outer mold line of the CS near the aft struts affected predicted booster separation clearances. Flex motion was accounted for in the EVE calculations by computing, in POST2, the flexible node displacement and rotation at the attachment point locations, and further translating and rotating the relevant geometry models by that amount.

To illustrate the importance of considering flexible body dynamics on forward attachment clearances, two Monte Carlo analyses were run, one with vehicle flexibility effects, and a second rigid case with flexible models deactivated. Figure 10 compares the -3σ forward attachment and aft diagonal strut clearance results for both cases. At the forward attachment, the effect of flexible alternates between increasing and decreasing the amount of clearance relative to the rigid body case. During the first ~0.1 second, when the SRB’s forward attach ball is moving out of the socket fitting on the CS, the -3σ clearance is reduced relative to the rigid body case. The effect of flex on the SRB aft diagonal strut clearance is smaller, but a similar alternating increasing/decreasing effect

is evident.

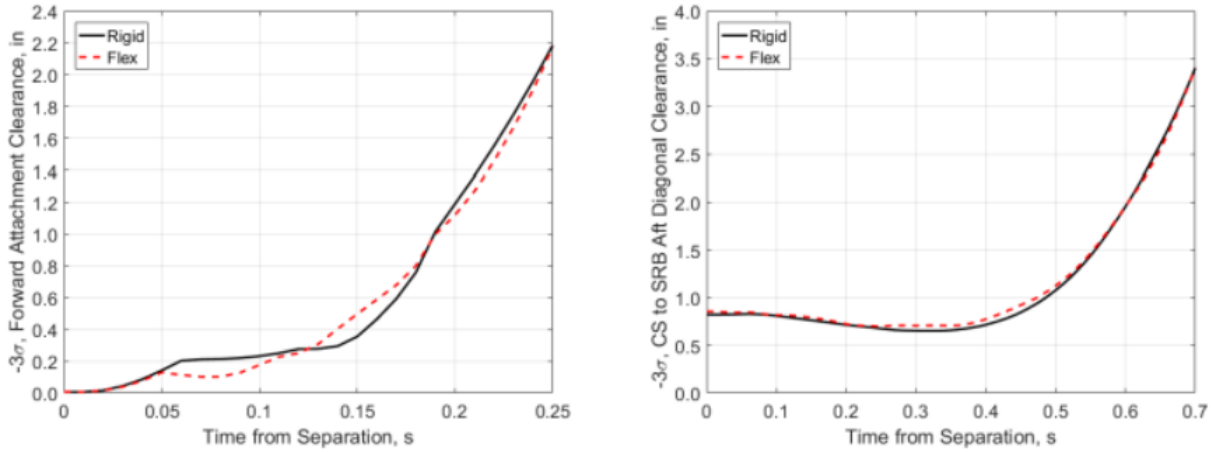

Figure 10. Effect of flexible body dynamics on forward and aft attachment clearances during booster separation.

3.3 SM Panel Separation

After booster separation, the next separation event is that of the SM panels. The SM panels encapsulate and protect the SM solar arrays during launch and must be jettisoned prior to the arrays being deployed. Each panel is attached to the SM via two hinges located at the panel base. Panel push-off is triggered by a jettison signal from the navigation computer when the on-board dynamic pressure estimate drops below 0.40 psf. The push-off is achieved by two preloaded springs located near the base of each panel, on either side of each panel centerline. The panel deployment rate when considering the mechanical and aerodynamic forces imparted on the panel is approximately 60° in 1.5 sec. An example of the MPCV SM panels during separation is shown in Figure 11.

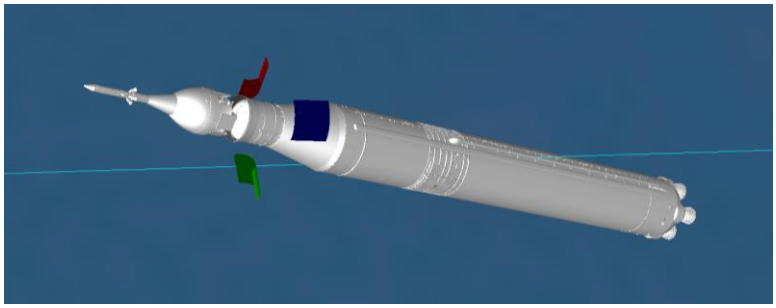

Figure 11. SM Panel separation simulated in EVE. Panels have just separated from the hinges and are in the near-field aerodynamic regime.

Accurate calculation of the SM panel trajectories required additional modeling fidelity to simulate the rotation of the panels on the hinges, and to account for the complex aerodynamic effects when panels were in proximity of the CS. Panel rotation was modeled using the Constraint Force Equation (CFE) methodology, which is available as an add-on module to POST2 to solve constrained motion problems, which occur when multiple bodies are connected by joints and the relative motion between the bodies is constrained in one or more translational and/or rotational degrees of freedom. Using the CFE approach, internal forces/moments acting at the joints connecting multiple bodies are computed and then applied as additional equal and opposite external forces/moments on the connected bodies. In other words, multiple bodies are treated as though they are “free” but subjected to additional constraint forces/moments as well as the typical external forces and moments acting on that body (i.e., due to gravity, aerodynamics, propulsion, etc). The trajectory is then propagated in POST2. Once the connected bodies separate, the constraint forces/moments vanish, and the simulation proceeds in the usual manner. A detailed discussion of

the CFE methodology is presented in [9] and [10]. The CFE implementation was verified using the industry standard Automatic Dynamics Analysis of Mechanical Systems (ADAMS) tool [11].

While the freestream dynamic pressure at panel jettison is small, the aerodynamic forces and moments are significant enough to influence the trajectories of the separated panels. The panel separation dynamics are modeled through three different aerodynamic regimes:

1. **Attached/Hinged:** The panels are rotating about the hinges to a specified angle prior to their release. Panel-to-panel and panel-to-CS aerodynamic effects are modeled.
2. **Near-field:** The panels have separated from the hinges. Panel-to-panel aerodynamic effects are not included. Panel-to-CS aerodynamic effects are modeled.
3. **Far-field (panel alone):** The panels are in freestream flow. Panel-to-panel and panel-to-CS aerodynamic effects are no longer included.

The SM panel jettison aerodynamic database was developed by the SLS Program using the inviscid Cart-3D CFD flow solver. Aerodynamic coefficient uncertainties were also included. An example of Cart-3D generated pressure contours around the deflected panels is shown in Figure 12. The aerodynamics were integrated into POST2 and used in the NESC modeling.

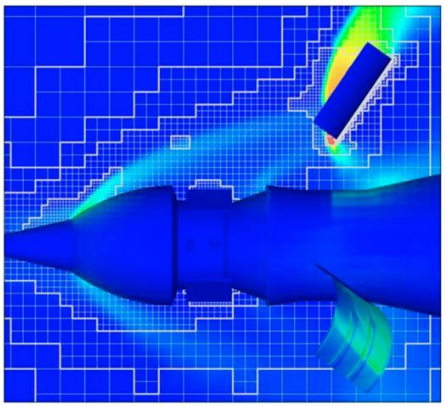

Figure 12. Example of CART-3D generated pressure contours.

Depending on the regime, the aerodynamic force and moment coefficients acting on the panels were a function of panel deployed angle, axial and radial separation distances from the CS, and roll/pitch/yaw Euler angles describing the panel orientations. For implementation of the aerodynamic database in the POST2 simulation, appropriate coordinate transformations were used to convert the aerodynamic forces from SLS coordinate system to panel local body-fixed coordinate system used in POST2 simulations.

To simulate the SM Panel separation, each panel was modeled as a separate 6-DOF body with its own mass, center of gravity, and inertia terms. The hinges for each panel were modeled in POST2 as a single one-dimensional rotational (pin) joint using the CFE module. The panel remains hinged until the rotation angle relative to the CS exceeds ~60 degrees. A nominal SM panel separation is shown in Figure 13. The three different aerodynamic regimes the panels experience during their separation is indicated by the color coding of the panel. Monte Carlo analyses were performed to quantify the variation in each panel's separation trajectory due to uncertainties in the panel aerodynamics, uncertainties in the SLS vehicle parameters, and expected variation in environmental parameters. A time history of each panel's proximity to the SLS stack was calculated using EVE for each dispersed case in the Monte Carlo analysis and used to quantify the panel's proximity statistical parameters.

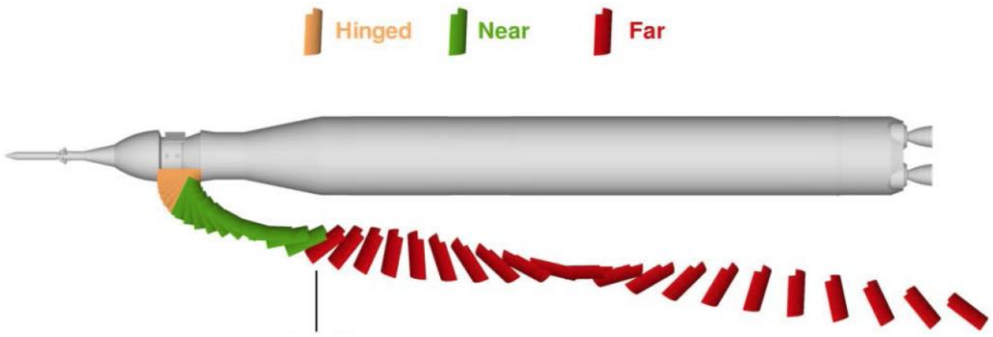

Figure 13. Nominal SM panel separation showing the three aerodynamic regimes that were modeled.

3.4 CS/ICPS Separation

The SLS CS fires until the SLS meets its orbital insertion target. Shortly after CS MECO, the SLS upper stage (US) is separated from the CS. The US consists of the ICPS, European Service Module (ESM), and Crew Module (CM). The US is joined to the CS through a tapered adapter referred to as the Launch Vehicle Stage Adapter (LVSA). The US is attached to the CS through a frangible joint between the upper end of the LVSA and the mid-section of the ICPS. At separation, the frangible joint is exploded, severing the connection between the ICPS and CS and a pneumatic actuator subsystem (PAS) pushes the stages apart. The PAS consists of 16 pneumatic actuators powered by two nitrogen gas tanks. The pneumatic actuators are mounted in pairs around the circumference of the LVSA. Figure 14 shows the location of the LVSA, ICPS, and CS/ICPS joint in the SLS stack, and the pneumatic actuator pairs mounted on the LVSA.

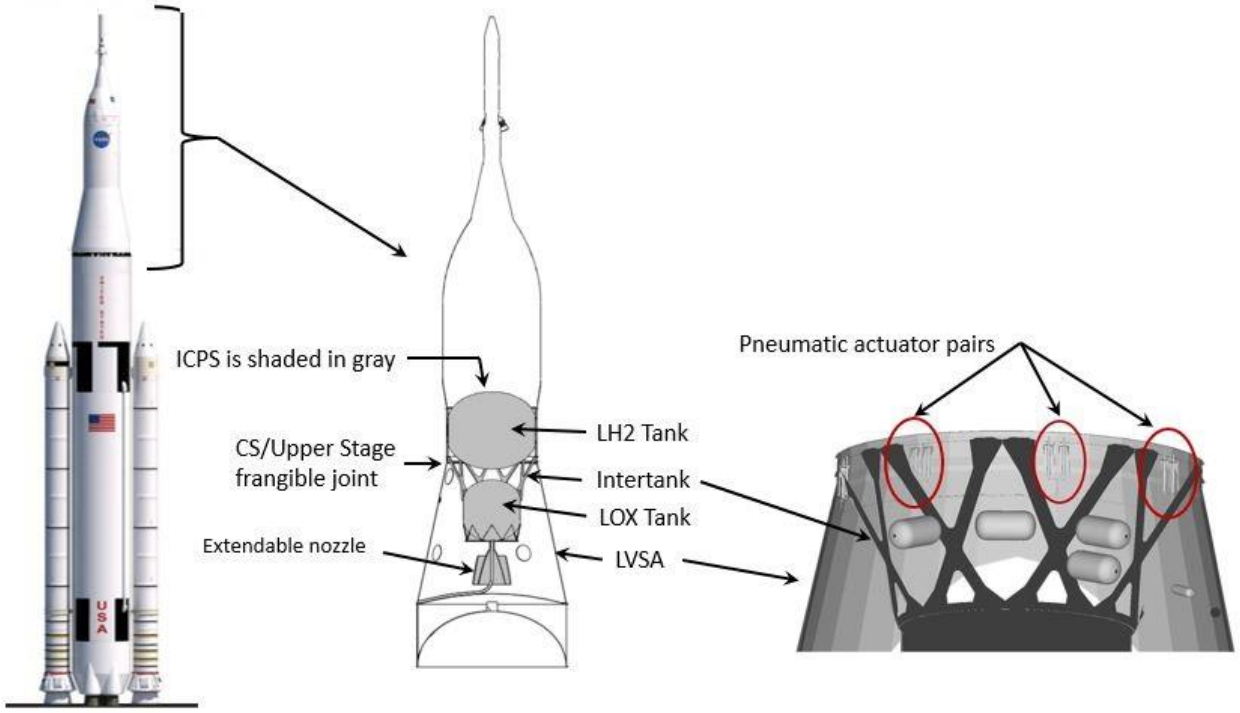

Figure 14. Location of key US elements on SLS vehicle stack and pneumatic actuators on the LVSA

The goal of the CS/ICPS separation analysis was to show analytically that the SLS Program's requirement for no recontact to occur between the ICPS and LVSA or any other part of the launch vehicle was met.

The POST2 simulation determined the dynamics of CS and US during the separation event that resulted from the interaction of the PAS actuators and umbilicals on the LVSA and ICPS. The POST2 dynamics provided a time history of each stage's 6-DOF state as well the relative 6-DOF state between the stages. An EVE proximity calculation coupled the POST2 6-DOF state time history with CAD models of the LVSA and ICPS to precisely orient their structural geometry relative to each other and determine the point of closest proximity between the stages' structural geometry throughout the separation event.

The POST2 simulation framework provided a means of integrating PAS specific models into the flight simulation. Specifically, models of the actuators attached to the LVSA, their associated contact surface on the ICPS, and a model of the PAS tank pressurization were integrated into the simulation. The actuator model represented the actuator's force as a function of stroke and tank pressure and represented the actuator's force line of action. The contact model represented the surface on which the actuator tip pushed. The model represented both the angle between the actuator's line of action and the bounds of the contact surface. The surface boundary represented the area on which the actuator could push. While the actuator's line of action intersected the contact area, the actuator's force acting on the contact surface was a function of the angle between the contact surface normal and the actuator's line of action. If the actuator's line of action did not intersect the contact area due to relative motion between the stages, then the actuator tip had slipped off the contact area and no longer applied the force to the ICPS. The tank pressurization model represented the tank pressure as a function of temperature.

Monte Carlo analyses were used to demonstrate the statistical parameters of the Program's requirement were met. Monte Carlo analyses were performed for both a fully operational PAS and a PAS with a single fault failure. Multiple failure scenarios were also analyzed. The Monte Carlo analyses incorporated the full set of the SLS vehicle related dispersions, environmental dispersions, and PAS parameter dispersions. The closest proximity/clearance between the ICPS and LVSA for an operational PAS Monte Carlo are shown in Figure 15.

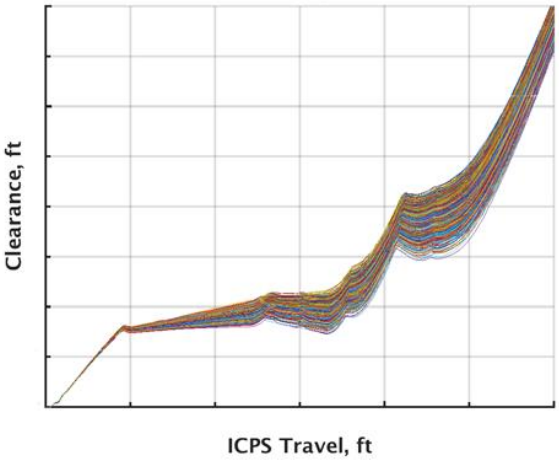

Figure 15. Separation clearance profiles between the ICPS and LVSA from Monte Carlo analysis.

3.5 ICPS/MPCV Separation

The nominal ICPS/MPCV separation occurs soon after the Trans-Lunar Injection (TLI) burn that places the MPCV on its trajectory to the moon. Spring loaded mechanisms called Space Craft Separation Mechanisms (SCSMs) are used to separate the ICPS from the MPCV. There are six SCSM units distributed around the circumference of the Spacecraft Adaptor (SA) used to join the ICPS to the MPCV. Each unit consists of a reaction bracket mounted to the MPCV, a base mounted to the SA, two springs with extension guides compressed between the base and reaction bracket, and a pyrotechnic retention bolt. During separation, the pyrotechnic retention bolt is activated severing the bolted joint and allowing the springs to push the stages apart. As the stages separate, lanyards are used to disconnect electrical connectors. The disconnection imparts an impulse force to

the ICPS and MPCV.

The goal of performing the ICPS/MPCV separation analysis was to show analytically that the Orion Program's no-recontact and a tip-off rate requirements were met. NESC analysis results were compared to results from an analysis performed by the MPCV Program as a means of providing verification of the Program's analysis. The ICPS/MPCV separation was simulated in POST2. The POST2 simulation determined full 6-DOF dynamic states of the ICPS and MPCV. The ICPS and MPCV dynamics were transferred to EVE where proximity was computed based on CAD models of the SCSM, SA, ESM, and ESM KOZ, which was a buffer zone around the ESM nozzle and other aft components.

The SCSM units were modeled in POST2 in a similar manner as the CS/ICPS PAS actuators. The SCSM model represents the line of action of its springs and the surface area on which the springs push. It also models the lateral stiffness the spring extension guides provide during the separation. The SCSM used springs rather than pneumatic actuators, thus the SCSM force versus displacement characteristics were based on a linear spring rate. The lanyard disconnection was modeled using the POST2 line/spring model in which lines between two vehicles can be defined with equal and opposite forces imparted to each vehicle along that line.

Monte Carlo analyses were used to demonstrate the Program's requirements were met. Monte Carlo analyses were performed for both a fully functional SCSM and SCSM with single and dual faults. In the Monte Carlo script, one spring was randomly selected to fail for a single fault failure. A dual fault failure scenario was modeled similarly by randomly failing two springs. Figure 16 shows the MPCV geometries, including the KOZ and SCSM springs representing the ICPS geometry and the closest proximity/clearance between those geometries for a functional SCSM.

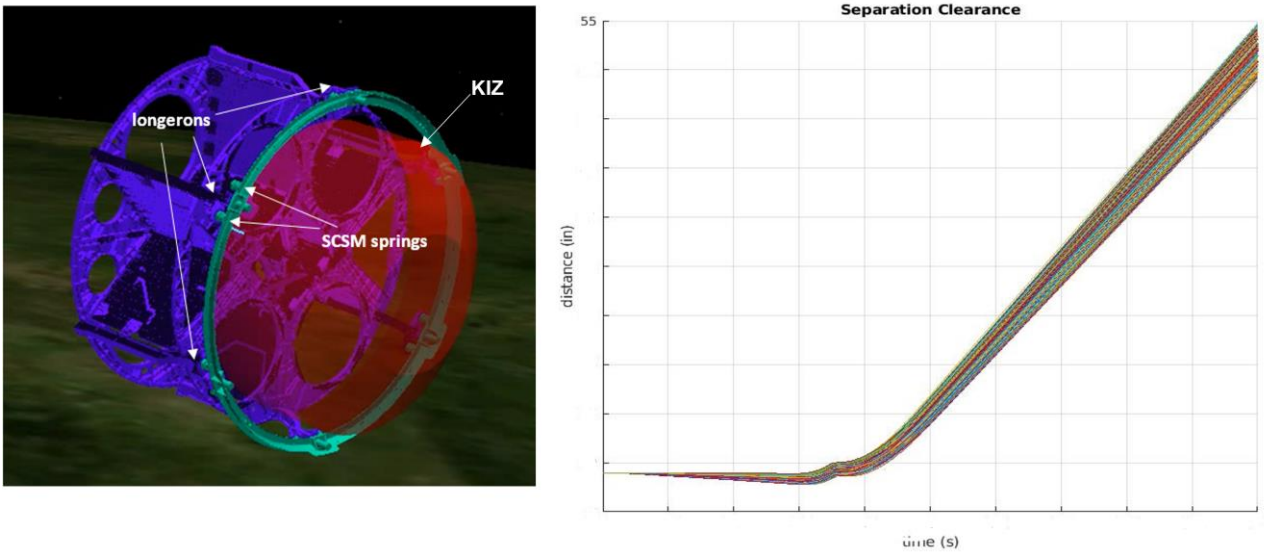

Figure 16. MPCV geometry ICPS KOZ (left); Monte Carlo profiles of separation clearances (right).

4 Summary

As part of its mission to ensure the safety and mission success of NASA's high-risk projects, the NESC assembled a subject matter expert team to develop and maintain an independent modeling, simulation, and separation analysis capability for the SLS vehicle. The effort was initiated early in

the SLS design cycle and has resulted in a versatile simulation architecture that has been used to perform detailed IV&V analyses for the critical ascent separation events for the Artemis I mission.

To create this architecture, the team developed an end-to-end 6-DOF simulation of the SLS ascent trajectory using the industry standard trajectory optimization and simulation code, POST2. The simulation included a comprehensive set of models capable of capturing the complexity of the SLS vehicle systems and dynamics that include GN&C flight software, structural flexibility, propellant slosh effects, and separation mechanisms. The simulation provides a versatile framework capable of simulating the entire ascent and performing in-depth analyses on individual separation events. To evaluate separation performance, dispersed Monte Carlo simulation analyses were conducted and separation clearances were computed using the visual software environment, EVE, to "drive" detailed vehicle geometry models with time-based dynamics data from the simulation and compute the minimum distance between separating bodies.

This paper described five different separation analyses that were performed throughout the SLS design, verification, and flight readiness cycles: 1) analysis of liftoff clearance between the SLS and launch/ground support structures; 2) separation of the SRBs from the CS; 3) SM panel jettison; 4) separation of the ICPS from the CS after MECO; and 5) MPCV/ICPS separation after TLI. All of these analyses were performed using the same end-to-end simulation architecture which aided in including the impact of the ascent and separation events prior to the event under consideration. Details were provided about additional simulation models that had to be added to adequately address issues specific to each separation event (booster separation aerodynamics, SM panel hinge joints, etc.). To address a need for adaptability, the architecture included a means of activating or deactivating simulation models so that modeling fidelity could be tailored to the specific analysis being performed.

There were numerous lessons learned over the course of this assessment. First, the independent simulation architecture developed by the NESC team provided high-fidelity verification of analysis which increased confidence in the Program's analysis results. The simulation fidelity was sufficient to accurately capture the separation dynamics and provide independent verification that the Program separation requirements were met. In addition, by initiating this effort early in the SLS development cycle, the NESC was able to assemble an in-house expertise that could evolve and became more complex as the system matured. This provided an independent analysis capability that could be leveraged to perform special studies on an as-needed basis. Finally, by developing the simulation and incorporating models independently, the NESC gained insight and was better positioned to understand and challenge assumptions and results in a way that would not be possible by simply running or inspecting Program simulation tools. The simulation architecture proved useful for Artemis I and provides a basis for modeling ascent and separation analyses for future Artemis flights.

5 Acknowledgements

The authors would like to acknowledge Jill Prince and Dan Yuchnovicz for their leadership of the assessment team, Steve Derry and John Davidson for help with model implementation and simulation verification, and Stuart Rogers for the booster separation CFD plot shown in Figure 9.

6 References

[1] Gilbert, M. G., "Purpose, Principles and Challenges of the NASA Engineering and Safety Center", 8th IAASS Conference "Safety First, Safety for All," May 18-20, 2016, Melbourne, FL.

[2] Tartabini, P., Starr, B., Gumbert, C., Ivanov, M., and Straus, W, "Ares I-X Separation and Reentry Trajectory Analyses," AIAA 2011-6462, *AIAA Atmospheric Flight Mechanics Conference*, Portland, OR, 2011.

[3] Way, D., Dutta, S., Zumwalt, C., and Blette, D., "Assessment of the Mars 2020 Entry, Descent and Landing Simulation," AIAA-2022-0421, *AIAA SCITECH 2022 Forum*, San Diego, CA, 2022.

[4] Tartabini, P., Munk, M., and Powell, R., "The Development and Evaluation of an Operational Aerobraking Strategy for the Mars 2021 Odyssey Orbiter," AIAA 2002-4537, *AIAA/AAS Astrodynamics Specialist Conference and Exhibit*, Monterrey, CA, 2002.

[5] "Subversion Web Page", 2023, https://subversion.apache.org/docs/

[6] "Jenkins Web Page", 2023, https://www.jenkins.io/

[7] Tapley, B, Ries, J, Bettadpur, S, Chambers, D, Cheng, M, Condi, F, Gunter, B, Kang, Z, Nagel, P, Pastor, R, Pekker, T, Poole, S, and Wang, F, "GGM02 – An Improved Earth Gravity Model for GRACE," *Journal of Geodesy*, 2005. DOI 10.1007/s00190-005-0480-z.

[8] NPR 7150.2, "NASA Software Engineering Requirements", https://nodis3.gsfc.nasa.gov/displayDir.cfm?t=NPR&c=7150&s=2B

[9] Tartabini, P., Roithmayr, C., Toniolo, M., Karlgaard, C., and Pamadi, B., "Modeling Multibody Stage Separation Dynamics Using Constraint Force Equation Methodology," *Journal of Spacecraft and Rockets*, Vol. 48, No. 4, 2011, pp. 573-583.

[10] Pamadi, B., Tartabini, P., Toniolo, M., Roithmayr, C., Karlgaard, "Application of Constraint Force Equation Methodology for Launch Vehicle Stage Separation," *Journal of Spacecraft and Rockets*, Vol. 50, No. 1, 2013, pp. 191-205.

[11] Ortiz, J, Introduction to ADAMS/Solver C++, May 2011. (PDF) Adams Solver Guide - DOKUMEN.TIPS.